Please cite this article in press as: Usmani et al., *De novo* and bi-allelic variants in *AP1G1* cause neurodevelopmental disorder with developmental delay, intellectual dis..., The American Journal of Human Genetics (2021), https://doi.org/10.1016/j.ajhg.2021.05.007

REPORT

De novo and bi-allelic variants in *AP1G1* cause neurodevelopmental disorder with developmental delay, intellectual disability, and epilepsy

Muhammad A. Usmani,[1,2] Zubair M. Ahmed,[1,3] Pamela Magini,[4] Victor Murcia Pienkowski,[5] Kristen J. Rasmussen,[6] Rebecca Hernan,[7] Faiza Rasheed,[8] Mureed Hussain,[1] Mohsin Shahzad,[2] Brendan C. Lanpher,[6] Zhiyv Niu,[6,9] Foong-Yen Lim,[10] Tommaso Pippucci,[4] Rafal Ploski,[5] Verena Kraus,[11] Karolina Matuszewska,[12,13] Flavia Palombo,[4,14] Jessica Kianmahd,[15] UCLA Clinical Genomics Center, Julian A. Martinez-Agosto,[15,16,17] Hane Lee,[16,18] Emma Colao,[19] M. Mahdi Motazacker,[20] Karlla W. Brigatti,[21] Erik G. Puffenberger,[21] S. Amer Riazuddin,[22] Claudia Gonzaga-Jauregui,[23] Wendy K. Chung,[7,24] Matias Wagner,[25,26] Matthew J. Schultz,[6] Marco Seri,[4,27] Anneke J.A. Kievit,[28] Nicola Perrotti,[29] J.S. Klein Wassink-Ruiter,[30] Hans van Bokhoven,[31] Sheikh Riazuddin,[2,32] and Saima Riazuddin[1,3,*]

Summary

Adaptor protein (AP) complexes mediate selective intracellular vesicular trafficking and polarized localization of somatodendritic proteins in neurons. Disease-causing alleles of various subunits of AP complexes have been implicated in several heritable human disorders, including intellectual disabilities (IDs). Here, we report two bi-allelic (c.737C>A [p.Pro246His] and c.1105A>G [p.Met369Val]) and eight *de novo* heterozygous variants (c.44G>A [p.Arg15Gln], c.103C>T [p.Arg35Trp], c.104G>A [p.Arg35Gln], c.229delC [p.Gln77Lys*11], c.399_400del [p.Glu133Aspfs*37], c.747G>T [p.Gln249His], c.928−2A>C [p.?], and c.2459C>G [p.Pro820Arg]) in *AP1G1*, encoding gamma-1 subunit of adaptor-related protein complex 1 (AP1γ1), associated with a neurodevelopmental disorder (NDD) characterized by mild to severe ID, epilepsy, and developmental delay in eleven families from different ethnicities. The AP1γ1-mediated adaptor complex is essential for the formation of clathrin-coated intracellular vesicles. *In silico* analysis and 3D protein modeling simulation predicted alteration of AP1γ1 protein folding for missense variants, which was consistent with the observed altered AP1γ1 levels in heterologous cells. Functional studies of the recessively inherited missense variants revealed no apparent impact on the interaction of AP1γ1 with other subunits of the AP-1 complex but rather showed to affect the endosome recycling pathway. Knocking out *ap1g1* in zebrafish leads to severe morphological defect and lethality, which was significantly rescued by injection of wild-type *AP1G1* mRNA and not by transcripts encoding the missense variants. Furthermore, microinjection of mRNAs with *de novo* missense variants in wild-type zebrafish resulted in severe developmental abnormalities and increased lethality. We conclude that *de novo* and bi-allelic variants in *AP1G1* are associated with neurodevelopmental disorder in diverse populations.

Clathrin-coated vesicles mediate intra-organelle protein trafficking in living cells.[1] Adaptor proteins (APs) are required for the assembly, cargo sorting, and vesicular transport among various organelles, including endosomes, lysosomes, trans-Golgi networks (TGNs), and the plasma membrane.[1–4] Ubiquitously expressed AP complexes,

[1]Department of Otorhinolaryngology Head and Neck Surgery, School of Medicine, University of Maryland, Baltimore, MD 21201, USA; [2]Department of Molecular Biology, Shaheed Zulfiqar Ali Bhutto Medical University, Islamabad 44000, Pakistan; [3]Department of Molecular Biology and Biochemistry, School of Medicine, University of Maryland, Baltimore, MD 21201, USA; [4]U.O. Genetica Medica, IRCCS Azienda Ospedaliero-Universitaria di Bologna, Via Albertoni 15, Bologna, Italy; [5]Department of Medical Genetics, Medical University of Warsaw, 02-106 Warsaw, Poland; [6]Department of Laboratory Medicine and Pathology, Mayo Clinic, Rochester, MN 55905, USA; [7]Department of Pediatrics, Columbia University, New York, NY 10032, USA; [8]Centre of Excellence in Molecular Biology, University of the Punjab, Lahore 54500, Pakistan; [9]Department of Clinical Genomics, Mayo Clinic, Rochester, MN 55905, USA; [10]Division of Pediatric Surgery, Cincinnati Children's Hospital Medical Center, Cincinnati, OH 45229, USA; [11]Department of Pediatrics, Klinik für Kinder- und Jugendmedizin, München Klinik Schwabing und Harlaching, Klinikum Rechts der Isar der Technischen Universität Munich, Munich, Germany; [12]Department of Medical Genetics, University of Medical Sciences, 60-806 Poznan, Poland; [13]Centers for Medical Genetics GENESIS, Grudzieniec, 60-406 Poznan, Poland; [14]IRCCS Istituto delle Scienze Neurologiche di Bologna, Programma di Neurogenetica, 40139 Bologna, Italy; [15]Department of Pediatrics, David Geffen School of Medicine, University of California, Los Angeles, Los Angeles, CA 90095, USA; [16]Department of Human Genetics, David Geffen School of Medicine, University of California, Los Angeles, Los Angeles, CA 90095, USA; [17]Department of Psychiatry and Biobehavioral Sciences, David Geffen School of Medicine, University of California, Los Angeles, Los Angeles, CA 90095, USA; [18]Department of Pathology and Laboratory Medicine, David Geffen School of Medicine, University of California, Los Angeles, Los Angeles, CA 90095, USA; [19]Medical Genetics Unit, Mater Domini University Hospital, 88100 Catanzaro, Italy; [20]Amsterdam Laboratory of Genome Diagnostics, Academic Medical Center, Meibergdreef 9, 1105 AZ Amsterdam, the Netherlands; [21]Clinic for Special Children, Strasburg, PA 17579, USA; [22]The Wilmer Eye Institute, Johns Hopkins University School of Medicine, Baltimore, MD 21287, USA; [23]Regeneron Genetics Center, Tarrytown, NY 10591, USA; [24]Department of Medicine, Columbia University, New York, NY 10032, USA; [25]Institute of Human Genetics, Klinikum rechts der Isar, Technical University of Munich, Munich, Germany; [26]Institute of Neurogenomics, Helmholtz Zentrum München, Neuherberg, Germany; [27]Medical Genetics Unit, Department of Medical and Surgical Sciences, University of Bologna, 40138 Bologna, Italy; [28]Clinical Genetics, Erasmus MC, University Medical Center Rotterdam, 3015 GD Rotterdam, the Netherlands; [29]Department of Health Sciences, University of Catanzaro Magna Graecia, 88100 Catanzaro, Italy; [30]Department of Genetics, University of Groningen, University Medical Center Groningen, P.O. box 30.001, 9700 RB Groningen, the Netherlands; [31]Department of Human Genetics, Donders Institute for Brain, Cognition and Behaviour, Radboud University Medical Center, P.O. box 9101, 6500 HB Nijmegen, the Netherlands; [32]Jinnah Burn and Reconstructive Surgery Center, Allama Iqbal Medical College, University of Health Sciences, Lahore 54550, Pakistan

*Correspondence: sriazuddin@som.umaryland.edu

https://doi.org/10.1016/j.ajhg.2021.05.007.

composed of four interacting AP subunits, are classified into five cytosolic sub-families (AP-1–AP-5). Each of these cytosolic heterotetramers is unique in its sub-cellular targeting and cargo selection.[2] In humans, the AP-1 complex is composed of two large beta-adaptin (β) and gamma-adaptin (γ) subunits, one mu-1 (μ) subunit, and one small chain sigma (σ) subunit.[5,6] AP-1 complexes are involved in cargo sorting among endosomes, lysosomes, and TGNs in eukaryotic cells[7,8] and mediate basolateral sorting in polarized epithelial cells[9–12] and transport of transmembrane proteins to somatodendritic domains in neurons.[13–15] Loss of AP-1 complex subunits (γ1, β1, μ1, or σ1) in murine models results in either prenatal lethality or cause severe growth deficits,[9,13,16–18] highlighting their crucial role in organ development and associated functions. In humans, impaired functions of various subunits of AP complexes have been associated with severe inherited disorders. For instance, recessive loss-of-function variants in *AP1B1* cause a multi-organ disorder (MIM: 242150) with clinical manifestations including enteropathy, hearing impairment, peripheral neuropathy, ichthyosis, keratodermia, photophobia, epileptic encephalopathy, and intellectual disability (ID).[19,20]

ID affects around 3% of world population.[21] Recognized genetic factors contribute to the etiology of 25%–50% of ID cases, but the identification of disease-causing variants and genes has been long impeded by the extreme genetic heterogeneity.[22,23] Here, through combined clinical, genetics, biochemical, and imaging efforts, we have identified and functionally characterized two homozygous missense variants in two families of Pakistani and Italian origin and eight different *de novo* heterozygous variants in AP-1 subunit, *AP1G1* (MIM: 603533), associated with moderate to severe ID in nine families (Figure 1).

After the approval of study protocols, developed according to the World Health Organization's Declaration of Helsinki (2013), from the institutional review boards of all the participating institutions, written informed consents were obtained from all the participating adults and guardians of affected individuals and minors, while minors (ages 12 to 17 years) also signed the assent forms. Genomic DNA was isolated from venous blood of participating individuals and was analyzed by whole-exome sequencing at their ascertaining institutes. After the identification of the potentially pathogenic variants, the participating investigators were connected through the GeneMatcher website.[24]

Collectively, we investigated eleven families with variants in *AP1G1* (GenBank: NM_001030007.2; Figure 1). Two bi-allelic homozygous missense variants (c.737C>A [p.Pro246His] and c.1105A>G [p.Met369Val]) were found in available affected individuals from two distinct families with Italian[25] (CPBO) and Pakistani (PKMR328) origins, respectively. Moreover, eight *de novo* heterozygous variants were identified in nine isolated affected individuals from nine families (Figure 1C, Table 1), including five missense (c.44G>A [p.Arg15Gln], c.103C>T [p.Arg35Trp], c.104G>A [p.Arg35Gln], c.747G>T [p.Gln249His], and c.2459C>G [p.Pro820Arg]), two frameshift (c.229delC [p.Gln77Lys*11] and c.399_400del [p.Glu133Aspfs*37]), and an intronic variant (c.928−2A>C [p.?]) that disrupts the canonical splice acceptor site (Figure 1D). In our cohort, two unrelated families from Poland and the United States (families 4 and 5) had the same p.Arg35Trp variant, while family 6 from the Netherlands had a different amino acid substitution at the same position (p.Arg35Gln), suggesting a possible mutation hot-spot. All the identified missense variants were predicted to substitute evolutionary conserved residues (Figure 1E).

These *AP1G1* variants were not found in control samples nor in publicly available various population databases, except for the homozygous c.1105A>G variant that has seven carriers listed in the gnomAD and an overall allele frequency of 1.668×10^{-5} (Table S1). According to the gnomAD constraint parameters, *AP1G1* is highly intolerant to variations and has a probability of intolerance to loss of function (pLI) score of 1 (LOEUF score: 0.2) and a missense *Z* score of 2.98, while the RVIS ExAC score is −0.76 with 5th percentile of intolerance.[26]

Table 1 summarizes the core clinical features of affected individuals with *AP1G1* variants, while Table S2 specifies developmental milestones. All individuals had neurodevelopmental disorder (NDD) including global developmental delay and ID, which varied in severity from mild to severe, except the affected individual of family 8, who died at the age of 22 days (Table 1). Family CPBO, enrolled from Italy, had one living affected individual (IV:2) with severe ID (HP: 0001249) and agenesis of corpus callosum (HP: 0001274). She requires significant supervision for activities of daily living. Her sister (IV:1; Figure 1A) had agenesis of corpus callosum and ornithine transcarbamylase deficiency and died at the age of 2 years. The other three siblings have IQ levels within normal age range. The parents of these individuals are first cousins (Figure 1A). Another consanguineous family, PKMR328, was enrolled from Central Punjab, Pakistan. At the time of ascertainment, three of the five affected individuals were alive, including two affected brothers (IV:1 and IV:2) and their uncle (III:11; Figure 1B). The two siblings showed moderate to severe ID (HP: 0002342) with early onset, aggressive behavior (HP: 0000718), speech delay (HP: 0000750), epilepsy (HP: 0001250), delayed childhood milestones (HP: 0001263), spasticity (HP: 0001257), and decreased body weight (HP: 0004325) and had joint laxity (HP: 0002761; Table 1). Affected individual IV:1 was unable to stand (HP: 0003698) or chew (HP: 0005216) his food at the age of 19 years. By parents' report, he died at age 21 years as a result of sudden cardiac arrest (HP: 0001695); however, clinical notes were not available to further assess the cause of his death. Three of the father's siblings, two of whom died at a young age, also have/had ID (Figure 1B). Similarly, all the probands with *de novo* variants in *AP1G1* (Figure 1C), except the index affected individual of family 8, who died at the age of 22 days, presented with

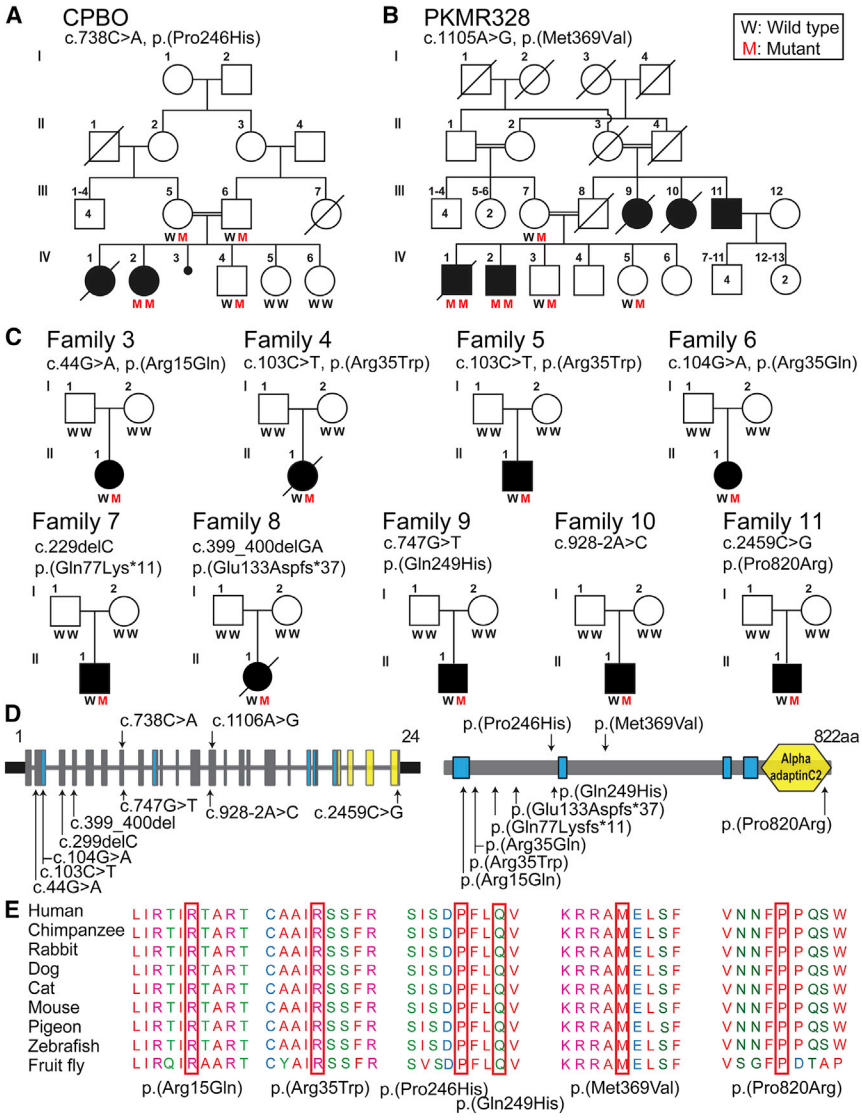

Figure 1. Homozygous as well as *de novo* variants in *AP1G1* cause neurodevelopment disorder (NDD) with intellectual disability and dysmorphic features

(A) Pedigree of Italian CPBO family segregating intellectual disability associated with a c.737C>A (p.Pro246His) variant in *AP1G1*. The filled symbols represent affected individuals, and a double horizontal line connecting parents represents a consanguineous marriage.

(B) Pedigree of Pakistani family PKMR328 segregating intellectual disabilities with dysmorphic features associated with a homozygous c.1105A>G (p.Met369Val) allele *AP1G1* variant.

(C) Pedigrees of nine outboard families segregating with *de novo* missense, frameshift, as well as splice variants.

(D) Schematic representation of human *AP1G1* gene and protein structures along with bi-allelic (above) and *de novo* (below) variants identified in families with NDD. Yellow hexagon represents Alpha adaptin C2 domain, while blue rectangles marked the exons encoding transmembrane domains.

(E) Clustal W alignment revealed high evolutionary conservation of residues mutated in families with NDD.

developmental delay, mild to moderate ID, speech delay, and behavioral problems (Tables 1 and S2). Some of these affected individuals also had hypotonia, epilepsy, and limb deformities (Table 1).

AP1G1 (MIM: 603533) encodes the 822 amino acid gamma-adaptin (γ) subunit of the AP-1 complex (AP1γ1). AP1γ1 is predicted to have four transmembrane domains followed by an alpha adaptin C2 domain at the carboxy terminus (Figure 1D), which is known to bind clathrin and other receptors in coated vesicles. The variants of AP1γ1 we report are predicted to have a deleterious impact on the encoded protein function by different *in silico* tools[27–31] (Table S1). Similarly, our 3D protein model using Phyre2 and PyMOL software (see web resources) and the protein structure available on the Protein Database (4HMY), as well as HOPE web server,[32] indicate a significant impact on the protein secondary structure, folding, and interactions due to size and/or charge differences between the wild-type (WT) and NDD-associated amino acid substitutions (Figure S1). Furthermore, the variant c.747G>T, found in family 9, besides substituting an invariant glutamine residue at position 249 with histidine (Figure 1E), is also predicted to affect exon splicing because of proximity to the exon-intron junction (Figure S2). We evaluated the effect of this variant *in vitro* by transfecting COS7 cells with constructs expressing WT or the c.747G>T variant harboring *AP1G1* exon 7 and examining the corresponding RNA splicing pattern. Indeed, the c.747G>T variant induced the skipping of exon 7 (Figure S2), most likely causing frameshift and premature truncation of the encoded protein.

To experimentally evaluate the effect of identified variants on the AP1γ1 protein level, we transiently transfected hemagglutinin (HA)-tagged clones with cDNAs of the WT and mutant (p.Arg15Gln, p.Arg35Trp, p.Arg35Gln, p.Gln77Lysfs*11, p.Glu133Aspfs*37, p.Pro246His, p.Met 369Val, and p.Pro820Arg) human *AP1G1* in HEK293T cells. 48 h after transfections, cells were harvested and analyzed for protein levels. Immunoblot with anti-HA antibodies revealed statistically significant differences in protein steady state levels in HEK293T cells. AP1γ1 harboring missense variants p.Arg15Glu, p.Arg35Trp, p.Pro246His, and p.Pro820Arg had significantly lower levels (*$p < 0.04$, ****$p < 0.0001$, **$p < 0.007$), while higher protein levels were observed for p.Arg35Gln and p.Met369Val

Please cite this article in press as: Usmani et al., *De novo* and bi-allelic variants in *AP1G1* cause neurodevelopmental disorder with developmental delay, intellectual dis..., The American Journal of Human Genetics (2021), https://doi.org/10.1016/j.ajhg.2021.05.007

Table 1. Clinical features of affected individuals harboring *AP1G1* variants

Family	CPBO	PKMR328		Family 3	Family 4	Family 5	Family 6	Family 7	Family 8	Family 9	Family 10	Family 11
Origin	Italy	Pakistan		Germany	Poland	USA	Dutch	Dutch	USA	USA	Dutch	USA
Variant	c.737C>A (p.Pro246His)	c.1105A>G (p.Met369Val)		c.44G>A (p.Arg15Gln)	c.103C>T (p.Arg35Trp)	c.103C>T (p.Arg35Trp)	c.104G>A (p.Arg35Gln)	c.299delC (p.Gln77Lys*11)	c.399_400del (p.Glu133Aspfs*37)	c.747G>T (p.Gln249His)	c.928−2A>C (p.?)	c.2459C>G (p.Pro820Arg)
Variant type	homozygous	homozygous		*de novo* heterozygous	*de novo* heterozygous	*de novo* heterozygous	*de novo* heterozygous	*de novo* heterozygous	*de novo* heterozygous	*de novo* heterozygous	*de novo* heterozygous	*de novo* heterozygous
ACMG classification	likely pathogenic	likely pathogenic		likely pathogenic	likely pathogenic	likely pathogenic	likely pathogenic	likely pathogenic	likely pathogenic	likely pathogenic	likely pathogenic	likely pathogenic
ACMG criteria	PS3, PM2	PS3, PM2		PS2, PM2, PP3	PS2, PM2, PP3	PS2, PM2, PP3	PS2, PM2, PP3	PS2, PM2, PP3	PS2, PM2, PP3	PS2, PM2, PP3	PS2, PM2, PP3	PS2, PM2, PP3
Individual[a]	III:5, 13 years	IV:2, 19 years	IV:I (died), 21 years	II:1, 7 years	II:1 (died), 4 years	II:1, 7 years	II:1, 18 years	II:1, 4 years	II:1 (died), 22 days	II:1, 6 years	II:1, 40 years	II:1, 14 years
Gender	female	male	male	female	female	male	female	male	female	male	male	male
Congenital anomalies	yes (agenesis of corpus callosum)	no	no	no	no	no	hearing loss	no	NA	pectus excavatum	NA	NA
Intellectual disability	severe	moderate	moderate	mild to moderate	moderate	moderate	mild	moderate	NA	mild	moderate, decreasing	yes
Speech delay	yes	yes	yes	yes	yes	yes	yes	yes	NA	yes	yes	yes
Developmental delay	yes	yes	yes	yes	yes	yes	yes	yes	NA	yes	yes	yes
Facial feature	high palate	prominent supraorbital ridges	–	normal	normal	eyelid hooding, long philtrum	no obvious dysmorphic features	frontal bossing, prominent forehead	NA	normal	turricephaly	NA
Hypotonia	severe	yes	severe	moderate truncal	yes	yes	yes; from few months of age	severe	NA	yes	no	NA
Epilepsy	no	yes	yes	yes	yes	single febrile seizure	no	no	NA	yes	no	NA
Spasticity	yes	yes	yes	no	yes	no	no	no	NA	no	no	NA
Behavioral problem	aggressive	–	aggressive	aggressive, hyperactivity	aggressive, hyperactivity	autism spectrum disorder, self-stimulatory and self-injurious behavior	depression, anxiety, disinhibition, and compulsive behavior	aggressive/ autism	NA	autism, hyperactivity, impulsivity, non-compliant	aggressive	yes
Eyes anomalies	hypertelorism epicanthus	hyperemic conjunctivae	no	no	strabismus	esotropia, anisometropia, amblyopia	no	no	NA	no	NA	NA

(*Continued on next page*)

Table 1. *Continued*

Family	CPBO	PKMR328	Family 3	Family 4	Family 5	Family 6	Family 7	Family 8	Family 9	Family 10	Family 11
Ear shape anomalies	low-set, posteriorly rotated ears	no	no	no	no	no	ear tag right ear	NA	no	NA	NA
Bony abnormalities	no	pectus excavatum	not evaluated	no	no	no	no	NA	no	pectus carinatum	NA
Vertebral anomalies	lumbar scoliosis	no	no	lumbar hyperlordosis	no	not known	no	NA	no	thoracal kyphosis	NA
Limb defects	no	joint laxity	joint laxity	short fingers, feet syndactyly II-III bilaterally	no	mild 5th finger clinodactyly, flat feet	widely spaced toes	no, small hands and feet	NA	long fingers and toes	long extremities

NA, not available; ACMG, American College of Medical Genetics and Genomics.
[a]Ages at the time of last clinical examination are given.

substitutions (*$p < 0.01$ and **$p < 0.007$, respectively) when compared to HA-AP1γ1^{WT} (Figure 2A). No protein was observed for frameshift variants p.Gln77Lysfs*11 and p.Glu133Aspfs*37 (Figure 2A), which could represent either nonsense-mediated decay (NMD) of the mRNA or protein degradation. To verify the latter mechanism, we treated HEK293T with either protease inhibitor MG132 (20 mM) or vehicle (0.5% DMSO). After 12 h of MG132 treatment, immunoblot revealed the production of truncated AP1γ1 proteins (Figure 2B), suggesting that p.Gln77Lysfs*11 and p.Glu133Aspfs*37 variants affect the stability of the encoded protein at least in *ex vivo* conditions and, thus, are loss-of-function alleles of *AP1G1*.

Next, we analyzed the effect of variants on the subcellular localization of AP1γ1. We first examined the protein level and targeting of endogenous AP1γ1 in rat hippocampal neuron and oligodendrocytes as well as in COS7 cells. In all these cell types, AP1γ1 is localized primarily in the perinuclear region (Figure S3). Next, HA- or GFP-tagged constructs were transiently transfected in COS7 cells (Figure 2C). 48 h after transfections, cells were fixed and immunostained with markers for clathrin heavy chain (CLTC), early endosomes (EEA1), late endosomes (RAB11), lysosomes (LAMP1), and TGN (mannosidase II). HA-AP1γ1^{WT} colocalized with clathrin-coated pits marked by CLTC (Figure 2C), recycling endosomes, lysosomes, and TGN (data not shown) predominantly at perinuclear area, which is consistent with the endogenous AP1γ1 protein level (Figure S3). No apparent difference in the perinuclear distribution of HA-AP1γ1$^{p.Pro246His}$ or HA-AP1γ1$^{p.Met369Val}$ was observed in transiently transfected COS7 cells compared with HA-AP1γ1^{WT} (Figure 2C), indicating that these variants apparently do not alter the incorporation of AP1γ1 in the AP-1 complex and the cellular distribution. Conversely, *de novo* missense variants HA-AP1γ1$^{p.Arg15Glu}$, HA-AP1γ1$^{p.Arg35Trp}$, and HA-AP1γ1$^{p.Arg35Gln}$ formed protein aggregates, while HA-AP1γ1$^{p.Pro820Arg}$ had diffuse localization throughout the cytoplasm (Figure 2C). Finally, constructs with frameshift variants generated very low fluorescent signals (Figure 2C), confirming immunoblot results.

Because affected individual-derived cell lines for all the families were not available, except for family 7, we evaluated possible deleterious interactions between WT AP1γ1 and proteins carrying *de novo* variants through *ex vivo* overexpression analysis. The GFP-tagged *AP1G1* WT (GFP-AP1γ1^{WT}) construct was co-transfected with HA-tagged *AP1G1* constructs harboring either WT, p.Arg15Gln, p.Arg35Trp, p.Arg35Gln, p.Pro246His, p.Met369Val, or p.Pro820Arg variants in HEK293T cells, followed by immunoblot analyses 48 h after transfection. Comparison of relative steady state levels of GFP-AP1γ1^{WT} protein co-transfected with HA-AP1γ1^{WT} or missense variants harboring AP1γ1, after normalization against house-keeping GAPDH protein levels, did not reveal any statistically significant differences (Figure 2D). Interestingly, immunofluorescence analysis of co-transfected cells showed that

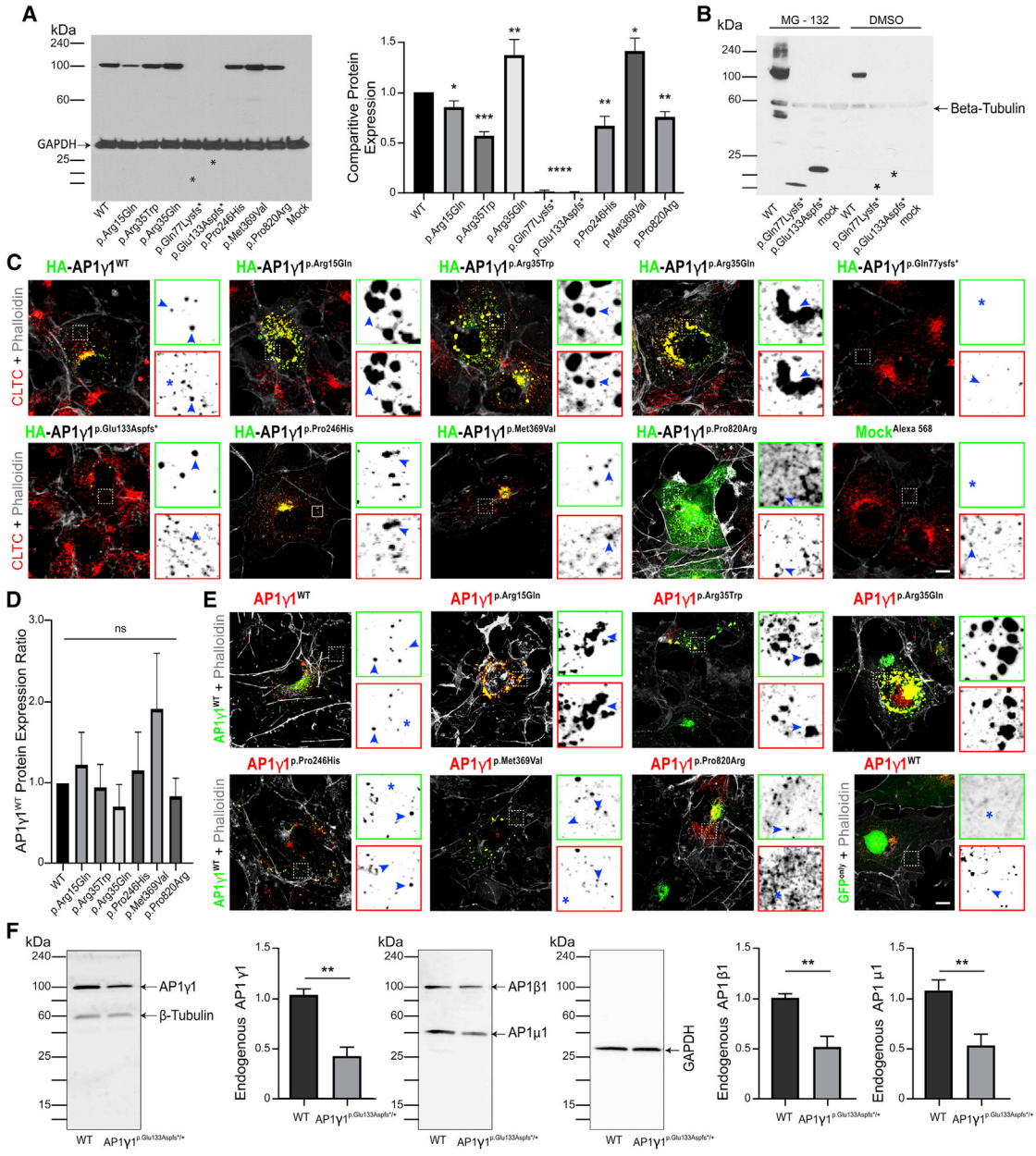

Figure 2. Impact of NDD-associated variants on AP1γ1 steady state level and targeting in heterologous cells

(A) Immunoblot revealed statistically significant differences in AP1γ1 steady state levels when overexpressed levels in HEK293T cells. AP1γ1 harboring missense variants p.Arg15Glu, p.Arg35Trp, p.Pro246His, and p.Pro820Arg had significantly decreased levels (*$p < 0.04$, **$p < 0.007$, ****$p < 0.0001$), while slightly increased protein levels were observed for AP1γ1 with p.Arg35Gln and p.Met369Val variants (*$p < 0.01$ and **$p < 0.007$, respectively) when compared with HA-AP1γ1^{WT}. In contrast, no detectable protein was observed for AP1γ1 harboring p.Gln77Lysfs*11 and p.Glu133Aspfs*37 frameshift variants.

(B) Protease inhibitor (MG132) assay. Levels of AP1γ1-truncated proteins due to p.Gln77Lysfs*11 and p.Glu133Aspfs*37 were significantly increased in HEK293T cells treated with MG132 (20 mM) for 12 h as compared to vehicle (0.5% DMSO)-treated cells.

(C) Confocal images of COS7 cells transfected with HA-AP1γ1 constructs and immunolabeled with CLTC (clathrin heavy chain marker) and phalloidin (actin marker). HA-tagged WT AP1γ1 (HA-AP1γ1^{WT}) colocalizes with clathrin-coated pits predominantly at perinuclear area. Similarly, no apparent differences in the distribution of HA-AP1γ1$^{p.Pro246His}$ or HA-AP1γ1$^{p.Met369Val}$ proteins were noted. However, AP1γ1 proteins harboring *de novo* missense variants (HA-AP1γ1$^{p.Arg15Glu}$, HA-AP1γ1$^{p.Arg35Trp}$, and HA-AP1γ1$^{p.Arg35Gln}$) form aggregates in the transfected cells, and HA-AP1γ1$^{p.Pro820Arg}$ had diffuse cytoplasmic localization. Finally, as anticipated from immunoblot analysis, no to very little protein was observed for AP1γ1 with frameshift variants (p.Gln77Lysfs*11 and p.Glu133Aspfs*37). The regions magnified with split channels next to each image are boxed. Scale bars: 10 μm and 2 μm (inset).

(D) Immunoblot revealed no statistically significant differences in steady state levels of GFP-AP1γ1^{WT} when co-transfected with HA-AP1γ1 harboring either p.Arg15Glu, p.Arg35Trp, p.Arg35Gln, p.Pro246His, p.Met369Val, or p.Pro820Arg missense variants in HEK293T cells.

(legend continued on next page)

only the AP1γ1 proteins with the *de novo* missense variants (p.Arg15Gln, p.Arg35Trp, and p.Arg35Gln) formed aberrant aggregates with AP1γ1^{WT} proteins (Figure 2E). These results suggest that heterozygous *de novo* missense variants could have a toxic dominant-negative effect.

Affected individual-derived primary fibroblast cell line was available for the proband harboring the p.Glu133Aspfs*37 *de novo* variant. As observed in transfected cells, immunoblot analysis revealed significant reduction in the AP1γ1 protein level in the affected individual fibroblast cells as compared to WT controls (Figure 2F). Unchanged levels of mutant *AP1G1* mRNA (Figure S4) confirmed that this variant affects protein stability and does not promote NMD. Besides AP1γ1, we also observed significant reduction (**$p < 0.005$) in the protein levels of AP1β1 and AP1μ1 in these cell lines (Figure 2F). Conversely, previous studies have shown that affected individual cell lines with loss-of-function alleles of AP1β1 also had reduced levels of AP1γ1.[20] Taken together, these results suggest that AP1γ1 and AP1β1 might stabilize each other in the AP-1 complex.

Next, through co-immunoprecipitation studies, we investigated the impact of AP1γ1$^{p.Pro246His}$ or AP1γ1$^{p.Met369Val}$ variants, which have no apparent impact on the localization of encoded proteins (Figures 2C and 2E), on the AP1γ1 homodimerization as well as interaction with other AP-1 complex subunits (Figure S5). HA-tagged AP1γ1^{WT}, AP1γ1$^{p.Pro246His}$, and AP1γ1$^{p.Met369Val}$ were transiently co-transfected in HEK293T cells in various combinations along with GFP-tagged AP1β1, AP1σ1, or AP1μ1. After 48 h, cells were harvested and co-immunoprecipitation was performed[33] with either anti-GFP affinity or HA agarose beads. WT as well as mutant AP1γ1 proteins were able to homodimerize (Figure S5). Similarly, no apparent difference in the interaction of p.Pro246His or p.Met369Val mutants with other AP-1 complex subunits was observed as compared to AP1γ1^{WT} (Figure S5). Although an *in vivo* scenario might be different, the results of these *ex vivo* studies suggest that the homozygous p.Pro246His or p.Met369Val alleles do not prevent the formation of the AP-1 complex.

Next, we studied whether the AP-1 complex formed by the p.Pro246His or p.Met369Val variants harboring AP1γ1 is fully functional. Previous studies have shown the involvement of AP1γ1 in transferrin recycling through endosomes.[34,35] Therefore, we investigated transferrin endosomal recycling pathway by pulse-chase analysis[36] in COS7 cells to evaluate the impact of p.Pro246His and p.Met369Val variants of AP1γ1 on the overall AP-1 complex function (Figure 3). Transferrin receptors use either fast (early endosomes) or slow routes (recycling endosomes) to recycle between intracellular compartments and the plasma membrane.[37] Both fast and slow processes were evaluated with fluorescently labeled transferrin (Alexa Fluor 568 Conjugate, Thermo Fisher Scientific) and COS7 cells transiently overexpressing GFP-tagged AP1γ1^{WT}, AP1γ1$^{p.Pro246His}$, or AP1γ1$^{p.Met369Val}$ (Figure 3). In cells overexpressing AP1γ1^{WT}, maximum colocalization of transferrin with EEA1 was observed right at 15 min pulse, while only a fraction of transferrin was localized with RAB11 at this time (Figures 3A and S6). Over time, transferrin localization in recycling endosomes increases with a decrease in early endosomes (Figure S7). After 1 h, very low transferrin levels were found in both early and recycling endosomes, indicating near complete removal/recycling of transferrin from the cells (Figures 3A and S7). Importantly, we did not observe any significant difference in the recycling of transferrin through early or recycling endosomes in cells overexpressing AP1γ1^{WT} as compared to non-transfected cells (Figure S8), suggesting that overexpression did not negatively impact the endosomes recycling process. When compared with cells expressing GFP-AP1γ1^{WT}, we did not observe any statistically significant difference in recycling of transferrin through early endosomes (marked by EEA1) in AP1γ1$^{p.Pro246His}$- or AP1γ1$^{p.Met369Val}$-expressing cells (Figure S6). However, when we analyzed the localization in recycling endosomes (marked by RAB11), we found significantly (***$p < 0.00001$, at 30 min) reduced transferrin in cells overexpressing AP1γ1$^{p.Pro246His}$ compared to neighboring non-transfected cells or cells overexpressing AP1γ1^{WT} (Figures 3A, 3B, and S7). These results suggest deficits in transferrin recruitment to recycling endosomes. In contrast, in cells overexpressing AP1γ1$^{p.Met369Val}$, transferrin recruitment to recycling endosomes was similar to AP1γ1^{WT} (Figure 3B). However, recycling out from the cells was delayed. At 45 and 60 min after pulse, significant (***$p < 0.00001$) transferrin positive recycling endosomes were observed when compared to AP1γ1^{WT} cells (Figure 3B). In short, *ex vivo* transferrin recycling assay indicates that the AP1γ1$^{p.Pro246His}$ variant affects the recruitment of vesicles from early endosomes to late endosomes, while the p.Met369Val allele interferes with the trafficking between recycling endosomes and plasma membrane, and thus both variants, homozygous in NDD-affected individuals, impair the function of the AP-1 complex.

To further gain insights about the pathogenetic mechanism of bi-allelic as well as *de novo* missense variants (p.Arg15Gln, p.Arg35Trp, p.Arg35Gln, p.Pro246His, p.Met369Val, and p.Pro820Arg) of AP1γ1 *in vivo*, we used a zebrafish model. Zebrafish has only one ortholog, which has 91% identity and 95% amino acid similarity with human AP1γ1. First, we obtained commercially (Wellcome Trust Sanger Institute, Stock#sa12746) available zebrafish

(E) Confocal images of COS7 cells co-transfected with GFP-AP1γ1^{WT} and HA- AP1γ1 constructs harboring NDD-associated missense variants. Only the HA- AP1γ1 with *de novo* missense variants, HA-AP1γ1$^{p.Arg15Glu}$, HA-AP1γ1$^{p.Arg35Trp}$ and HA-AP1γ1$^{p.Arg35Gln}$, impaired the distribution of GFP-AP1γ1^{WT} proteins and formed large protein aggregates in the cytoplasm.
(F) Immunoblot revealed statistically significant reduced AP1γ1, AP1β1, and AP1μ1 steady state levels in the AP1γ1$^{p.Glu133Aspfs*37}$ variant-harboring affected individual-derived primary fibroblast cells as compared WT control cells (**$p < 0.007$).

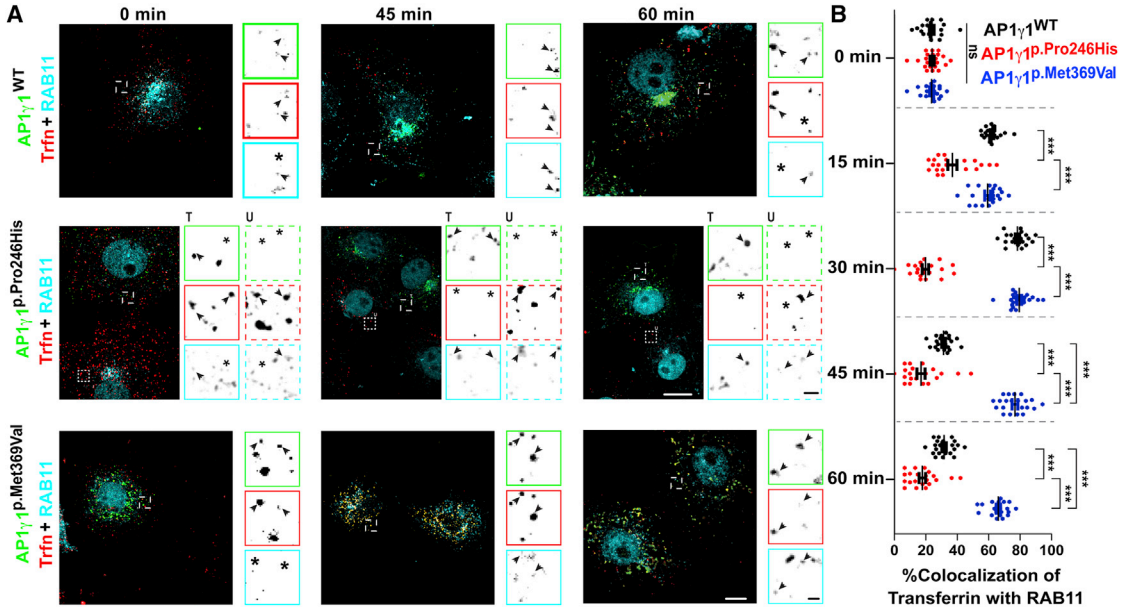

Figure 3. AP1γ1 NDD-associated variants impact the endosomal recycling pathway, evaluated via transferrin recycling

(A) COS7 cells transiently transfected with GFP-AP1γ1^{WT}, GFP-AP1γ1$^{p.Pro246His}$, or GFP-AP1γ1$^{p.Met369Val}$ and immunostained with RAB11 to mark the recycling endosomes. Cells were pulsed with transferrin and chased for time points shown in (B). Single channels are shown as inverted grayscale images with their respective channel color boxes. Colocalization is indicated with arrow heads and asterisks are indicating the absence of the respective marker. Representative images at time point 0 min (initiation of transferrin chase), 45 min, and 60 min are shown. Images for other studies' time points are given in Figure S4. White rectangles marked the area enlarged from transfected (T) or neighboring untransfected (U) cells.

(B) Quantification of colocalization pattern with ImageJ software at different time points revealed significant difference for both variants compared to WT protein. In cells transfected with AP1γ1^{WT}, most of the transferrin enters in recycling endosomes, as early as 15 min, and is recycled out after 30 min, while AP1γ1$^{p.Met369Val}$-transfected cells were unable to recycle transferrin through recycling endosomes, as colocalization of AP1γ1 with transferrin and RAB11 was observed even at 45 min (****$p < 0.00001$, Student's t test) and 60 min post chase. In contrast, transferrin was recycled out before 30 min (****$p < 0.00001$) through fast recycling route from cells transfected with AP1γ1$^{p.Pro246His}$, and very few transferrin-positive recycling endosomes were observed at later time points. Scale bars, 10 μm and 2 μm (inset).

mutant strain of *ap1g1* (*ap1g1*$^{-/+}$) that harbors a nonsense codon (p.Gln77*) within exon 2 (Figure S9A) and thus represents a functional null allele. We intercrossed heterozygous fish (*ap1g1*$^{+/-}$) to generate homozygous mutants. However, no homozygous *ap1g1*$^{-/-}$ mutants were recovered within the progeny of 1–2 months of age, most likely indicating the essential role of AP1γ1 in zebrafish survival. To test this hypothesis, we performed double-blind analysis of the zebrafish larvae, generated through *ap1g1*$^{+/-}$ × *ap1g1*$^{+/-}$ crosses. Investigators genotyping were not aware of the phenotype, and those harvesting larvae did not know the genotypes. All the larvae of these heterozygous crosses were imaged on sequential days (from 2 days post fertilization [dpf] until 7 dpf) followed by genotyping through Sanger sequencing (Figures 4A and S9). We processed all the images to measure the size of the brain sub-structures (forebrain, hindbrain, and midbrain) as well as total body length. When compared, larvae of all three genotypes, *ap1g1*$^{+/+}$, *ap1g1*$^{+/-}$, and *ap1g1*$^{-/-}$, were indistinguishable from each other and no statistically significant difference was observed in gross brain structures or total body length until 3 dpf (data not shown). By 4 dpf, we observed fluid accumulation (edema) in *ap1g1*$^{-/-}$ larvae, which became worse with age (Figures 4A and S6C), leading to eventual disintegration of the larvae. To further assess the survival of larvae, we performed Kaplan-Meier analysis. No significant survival deficits were observed in either *ap1g1*$^{+/+}$ or *ap1g1*$^{+/-}$ larvae, but after 4 dpf, *ap1g1*$^{-/-}$ larvae started dying and only 16% survived until 10 dpf (****$p < 0.0003$, Kaplan-Meier estimator, Student's t test), indicating the critical requirement of AP1γ1 for zebrafish survival (Figure 4B). Similar to zebrafish, a complete knockout of AP1γ1 function in mice is also embryonic lethal and *Ap1g1*$^{-/-}$ embryos only survive until early blastocyst stage.[16]

Importantly, we were able to significantly rescue the survival of *ap1g1*$^{-/-}$ larvae with human *AP1G1*^{WT} mRNA (250 pg) injected at the 1–2 cell stage (Figure 4C). The initial depletion stage is delayed to 7 dpf, and a significantly larger number of *ap1g1*$^{-/-}$ larvae survived (****$p < 0.0001$) through 10 dpf (Figures 4C and S7). Rescue of the survival phenotypes by injection of the human *AP1G1* mRNA with either c.737C>A (AP1γ1$^{p.Pro246His}$) or c.1105A>G (AP1γ1$^{p.Met369Val}$) variants was not statistically significant when compared with the uninjected *ap1g1*$^{-/-}$ larvae, further confirming the pathogenic nature of both variants (Figures 4C and S7). Nevertheless, as compared to uninjected *ap1g1*$^{-/-}$ larvae, we did observe delay in

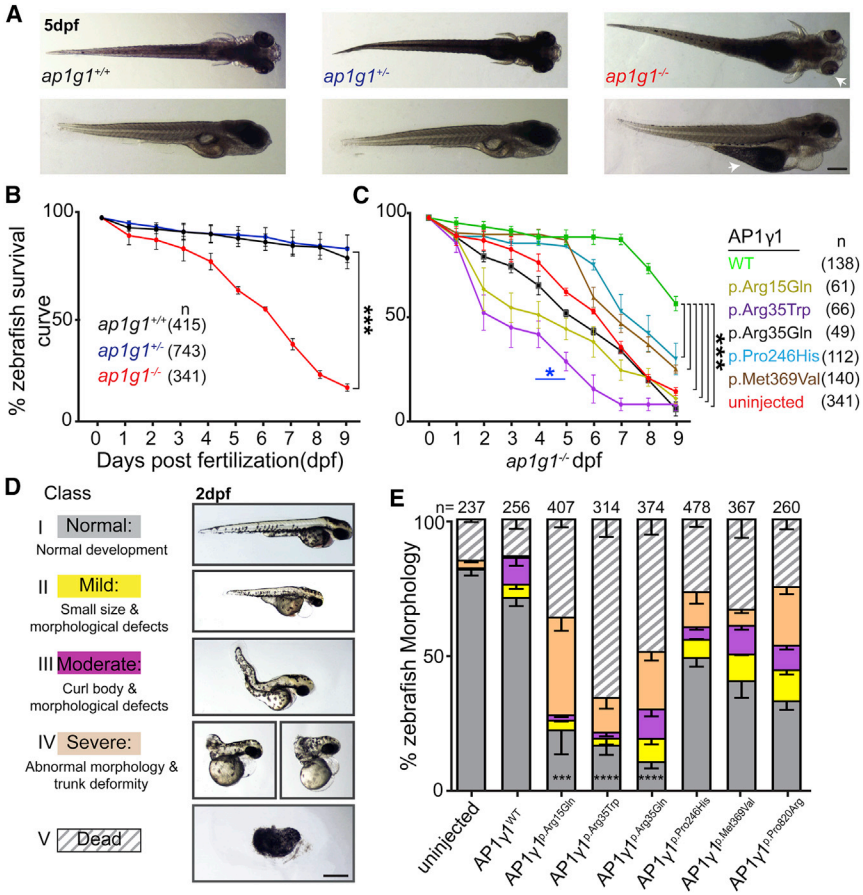

Figure 4. Ap1g1 is essential for zebrafish growth and survival

(A) Representative images of *ap1g1*$^{+/+}$, *ap1g1*$^{+/-}$, and *ap1g1*$^{-/-}$ larvae at 5 days post fertilization (dpf). Severe morphological defects, including edema, were observed in *ap1g1*$^{-/-}$ as early as 4 dpf.

(B) Kaplan-Meier curve showed only 16% of *ap1g1*$^{-/-}$ larvae survived until 10 dpf (****p < 0.0003, Kaplan-Meier estimator, Student's t test). No significant survival deficits were observed for *ap1g1*$^{+/-}$ larvae when compared with *ap1g1*$^{+/+}$, indicating that the Ap1g1 encoded by the single copy of *ap1g1* is sufficient for zebrafish survival.

(C) Human WT (*AP1γ1*^{WT}), but not the NDD-associated missense variants (p.Arg 15Gln, p.Arg35Trp, p.Arg35Gln, p.Pro246-His, and p.Met366Val) encoding mRNAs, rescued the edema phenotype and increased the survival of *ap1g1*$^{-/-}$ larvae (****p < 0.0001, Kaplan-Meier estimator, Student's t test). Blue asterisks marked statistically significant poor survival of the *de novo* variants injected larvae at 4 dpf when compared with uninjected *ap1g1*$^{-/-}$. Please see Figure S7 for additional experimental data graphs, including the microinjection of human *AP1G1* mRNA in all three genotypes (*ap1g1*$^{+/+}$, *ap1g1*$^{+/-}$, and *ap1g1*$^{-/-}$). Scale bar, 400 μm.

(D) *In vivo* microinjection of human *AP1G1* WT or mutant mRNAs in AB/TU wild-type zebrafish. Representative images of resulting phenotypes in developing larvae at 2 dpf. Larvae were categorized into five classes on the basis of their developmental morphology, edema, and survival.

(E) Only AP1γ1-harboring *de novo* missense variants, p.Arg15Glu, p.Arg35Trp, and Arg35Gln, showed dominant-negative impact and impaired the zebrafish development (***p < 0.001 and ****p < 0.0001, Student's t test) when compared with AP1γ1^{WT}-injected fish.

the initial depletion stage to day 5 in *ap1g1*$^{-/-}$ larvae injected with AP1γ1$^{p.Pro246His}$- or AP1γ1$^{p.Met369Val}$-encoding mRNAs (Figure 4C), suggesting that these variants do not cause complete loss of AP1γ1 function and might be hypomorphic alleles. In contrast, larvae injected with human *AP1G1* mRNA with either AP1γ1$^{p.Arg15Gln}$, AP1γ1$^{p.Arg35Trp}$, or AP1γ1$^{p.Arg35Gln}$ *de novo* variants had statistically significant poor survival even when compared to uninjected *ap1g1*$^{-/-}$ larvae, indicating their deleterious effect on protein function (Figures 4C and S7). Moreover, increased lethality of *ap1g1*^{WT} and *ap1g1*$^{+/-}$ larvae injected with either AP1γ1$^{p.Arg15Gln}$, AP1γ1$^{p.Arg35Trp}$, or AP1γ1$^{p.Arg35Gln}$ *de novo* variants was observed (Figure S10), supporting the dominant-negative nature of these variants.

Finally, larvae from AB/Tubingen (AB/TU) WT zebrafish at the 1–2 cells stage were injected with either human *AP1G1*^{WT} or missense variants (p.Arg15Gln, p.Arg35Trp, p.Arg35Gln, p.Pro246His, p.Met369Val, and p.Pro820Arg) harboring mRNAs (1 ng; Figure 4D). At 2 dpf, the zebrafish larvae were subdivided into five classes (Figure 4D) on the basis of their phenotype: normal (class I), mildly altered (class II), moderately altered (class III), severely altered (class IV), and dead larvae (class V). Larvae with mild phenotype (class II) only showed tail defect, while the other classes revealed moderate to severe developmental deficits, edema, and degeneration of larvae (Figure 4D). We did not observe statistically significant difference in the total number of larvae from AB/TU WT zebrafish in each of the five classes at 2 dpf after injection of human mRNAs encoding AP1γ1 with p.Pro246His or p.Met369Val NDD-associated variants (only in bi-allelic fashion) when compared with the total number of larvae in corresponding classes after injection of *AP1G1*^{WT} mRNA (Figure 4E). In contrast, the number of class I larvae was significantly decreased (t test, ***p < 0.001 and ****p < 0.0001) after injection of human mRNAs encoding AP1γ1 with p.Arg15Gln, p.Arg35Trp, or p.Arg35Gln *de novo* variants when compared with the total number of class I larvae found after injection of *AP1G1*^{WT} mRNA, while the class IV phenotype (abnormal morphology and trunk deformity) was significantly higher in larvae injected with AP1γ1 with the p.Pro820Arg variant (Figure 4E), further supporting the dominant-negative nature of these variants.

AP1γ1 is among the larger subunit of AP-1 complex with three distinct functional domains: head and trunk N-terminal domain, hinge domain, and the ear domain. AP1γ1 interacts with hundreds of accessory proteins directly or via other AP-1 subunits.[10,15,38,39] Among the

seven distinct proteins of the AP-1 complex, pathogenic variants in four of them have been associated with various human disorders, including ID.[19,20,40–42] Similarly, removal of many AP-1 complex subunits in animal models, including *Ap1g1*, results in embryonic lethality. For instance, $Ap1\sigma2^{-/-}$ mice have reduced motor coordination with impaired synaptic recycling and memory.[13] The $Ap1\mu2^{-/-}$ mice exhibit 50% lethality by 8 weeks of age, and there is significant growth retardation in the remaining survivors.[9] The $Ap1\mu1^{-/-}$ mice only survive until embryonic day 13.5.[17] Recent studies have shown involvement of AP1γ1 in immunodeficiencies[43,44] and carcinoma pathways.[45,46] The AP-1 adaptor complex is proven to be important for proper trafficking of vesicular proteins and is essential for development and function of several vital organs, including the brain. The AP-1 complex has been also implicated in the polarized sorting of somatodendritic proteins within the soma or retrograde retrieval from axons,[13–15] and interference with AP-1 complex function results in reduced number of synapses and morphological defects in dendritic spines.[15]

Our studies provide evidence for the essential role of AP1γ1 in the normal development and cognitive function in humans and growth in the zebrafish model. We identified *de novo* heterozygous and recessively inherited variants in *AP1G1* in eleven families with neurodevelopmental disorder. All the disease-associated variants, including missense alleles, are present within N-terminal half and affect the evolutionary conserved residues. The clinical phenotypes associated with homozygous and *de novo* heterozygous variants share several common neurodevelopmental abnormalities, including ID, epilepsy, developmental delay, speech delay, hyperactivity, and aggressive behavior. Our functional studies suggest that the disease mechanism for *de novo* missense variants could be toxic dominant negative and, for bi-allelic variants, partial loss of function. In zebrafish, removal of *ap1g1* significantly affected the development of larvae and resulted in reduced viability. Similar to humans and the zebrafish model, the *Ap1g1* mutant mice also displayed highly variable phenotype. Mice homozygous for a null mutation of *Ap1g1* died at embryonic day 3.5, and heterozygous mice displayed a reduced growth rate and impaired T cell development.[16] However, behavioral phenotype, neuronal function, or brain development was not evaluated in the heterozygous mice.[16] In contrast, mice homozygous for a hypomorphic allele (in-frame deletion of 6 bp) of *Ap1g1* are viable and exhibit multi-organs dysfunctions, including inner ear, retina, thyroid, and testes abnormalities, with reduced penetrance.[18] Around 70% of the *Ap1g1* hypomorphic mice had behavioral deficits, while hearing loss was noted in ~30% mutants,[18] potentially indicating the role of genetic background or other AP-1 complex proteins in modulating the phenotypes. Nevertheless, knockin mouse models would help elucidate the precise role of AP1γ1 in brain development and the mechanism of ID associated with identified variants.

Data and code availability

This study did not generate datasets or code.

Supplemental information

Supplemental information can be found online at https://doi.org/10.1016/j.ajhg.2021.05.007.

Acknowledgments

We are very thankful to the affected individuals and their families who have participated in this study. We would like to thank Drs. Elodie Richard and Saumil Sethna and Ms. Amama Ghaffar for their guidance and technical assistance. We also thank UMB Confocal Microscope Core facility and Dr. Joseph Mauban for the technical support. This work was supported by R01NS107428 (to S.R.), the EU FP7 Large-Scale Integrating Project Genetic and Epigenetic Networks in Cognitive Dysfunction (241995) (to H.v.B.), and the Higher Education Commission of Pakistan (NRPU project 10700) (to M. Shahzad). WES of the Italian family was funded by a "Fondazione del Monte" grant for application of clinical exome to the diagnosis of ultrarare/orphan inherited diseases (ID ROL: FDM/4021) (to M. Seri).

Declaration of interests

The authors declare no competing interests.

Received: October 7, 2020
Accepted: May 14, 2021
Published: June 7, 2021

Web resources

Allen Brain Atlas, https://portal.brain-map.org/
CADD, https://cadd.gs.washington.edu
Clustal Omega, Multiple Sequence Alignment, https://www.ebi.ac.uk/Tools/msa/clustalo/
ExAC, http://exac.broadinstitute.org
gnomAD, https://gnomad.broadinstitute.org
HOPE, https://www3.cmbi.umcn.nl/hope/
InterPro annotation, https://www.ebi.ac.uk/
MARRVEL, http://marrvel.org/
MutationTaster, http://www.mutationtaster.org
Online Mendelian Inheritance in Man, https://www.omim.org/
PolyPhen-2, http://genetics.bwh.harvard.edu/pph2
PROVEAN, http://provean.jcvi.org
REVEL, https://sites.google.com/site/revelgenomics/
RVIS, http://genic-intolerance.org/

References

1. Hirst, J., and Robinson, M.S. (1998). Clathrin and adaptors. Biochim. Biophys. Acta *1404*, 173–193.
2. Robinson, M.S. (2015). Forty Years of Clathrin-coated Vesicles. Traffic *16*, 1210–1238.
3. Ohno, H. (2006). Clathrin-associated adaptor protein complexes. J. Cell Sci. *119*, 3719–3721.
4. Popova, N.V., Deyev, I.E., and Petrenko, A.G. (2013). Clathrin-mediated endocytosis and adaptor proteins. Acta Naturae *5*, 62–73.

5. Traub, L.M., Kornfeld, S., and Ungewickell, E. (1995). Different Domains of AP1 Adaptor complex are required for Golgi membrane binding and clathrine recruitment. J. Biol. Chem. *270*, 4933–4942.
6. Boehm, M., and Bonifacino, J.S. (2001). Adaptins: the final recount. Mol. Biol. Cell *12*, 2907–2920.
7. Seaman, M.N.J., Sowerby, P.J., and Robinson, M.S. (1996). Cytosolic and Membrane-associated Proteins Involved in the Recruitment of AP-1 Adaptors onto the Trans-Golgi Network. J. Biol. Chem. *271*, 25446–25451.
8. Li, X., Ortega, B., Kim, B., and Welling, P.A. (2016). A Common Signal Patch Drives AP-1 Protein-dependent Golgi Export of Inwardly Rectifying Potassium Channels. J. Biol. Chem. *291*, 14963–14972.
9. Hase, K., Nakatsu, F., Ohmae, M., Sugihara, K., Shioda, N., Takahashi, D., Obata, Y., Furusawa, Y., Fujimura, Y., Yamashita, T., et al. (2013). AP-1B-mediated protein sorting regulates polarity and proliferation of intestinal epithelial cells in mice. Gastroenterology *145*, 625–635.
10. Gonzalez, A., and Rodriguez-Boulan, E. (2009). Clathrin and AP1B: key roles in basolateral trafficking through trans-endosomal routes. FEBS Lett. *583*, 3784–3795.
11. Futter, C.E., Gibson, A., Allchin, E.H., Maxwell, S., Ruddock, L.J., Odorizzi, G., Domingo, D., Trowbridge, I.S., and Hopkins, C.R. (1998). In polarized MDCK cells basolateral vesicles arise from clathrin-γ-adaptin-coated domains on endosomal tubules. J. Cell Biol. *141*, 611–623.
12. Fölsch, H., Ohno, H., Bonifacino, J.S., and Mellman, I. (1999). A Novel Clathrin Adaptor Complex Mediates Basolateral Targeting in Polarized Epithelial Cells. Cell *99*, 189–198.
13. Glyvuk, N., Tsytsyura, Y., Geumann, C., D'Hooge, R., Hüve, J., Kratzke, M., Baltes, J., Boening, D., Klingauf, J., and Schu, P. (2010). AP-1/sigma1B-adaptin mediates endosomal synaptic vesicle recycling, learning and memory. EMBO J. *29*, 1318–1330.
14. Guardia, C.M., De Pace, R., Mattera, R., and Bonifacino, J.S. (2018). Neuronal functions of adaptor complexes involved in protein sorting. Curr. Opin. Neurobiol. *51*, 103–110.
15. Bentley, M., Decker, H., and Banker, G. (2012). The clathrin adaptor complex responsible for somatodendritic protein sorting. Neuron *75*, 742–744.
16. Zizioli, D., Meyer, C., Guhde, G., Saftig, P., von Figura, K., and Schu, P. (1999). Early embryonic death of mice deficient in γ-adaptin. J. Biol. Chem. *274*, 5385–5390.
17. Meyer, C., Zizioli, D., Lausmann, S., Eskelinen, E.L., Hamann, J., Saftig, P., von Figura, K., and Schu, P. (2000). μ1A-adaptin-deficient mice: lethality, loss of AP-1 binding and rerouting of mannose 6-phosphate receptors. EMBO J. *19*, 2193–2203.
18. Johnson, K.R., Gagnon, L.H., and Chang, B. (2016). A hypomorphic mutation of the gamma-1 adaptin gene (Ap1g1) causes inner ear, retina, thyroid, and testes abnormalities in mice. Mamm. Genome *27*, 200–212.
19. Alsaif, H.S., Al-Owain, M., Barrios-Llerena, M.E., Gosadi, G., Binamer, Y., Devadason, D., Ravenscroft, J., Suri, M., and Alkuraya, F.S. (2019). Homozygous Loss-of-Function Mutations in AP1B1, Encoding Beta-1 Subunit of Adaptor-Related Protein Complex 1, Cause MEDNIK-like Syndrome. Am. J. Hum. Genet. *105*, 1016–1022.
20. Boyden, L.M., Atzmony, L., Hamilton, C., Zhou, J., Lim, Y.H., Hu, R., Pappas, J., Rabin, R., Ekstien, J., Hirsch, Y., et al. (2019). Recessive Mutations in AP1B1 Cause Ichthyosis, Deafness, and Photophobia. Am. J. Hum. Genet. *105*, 1023–1029.
21. Anazi, S., Maddirevula, S., Faqeih, E., Alsedairy, H., Alzahrani, F., Shamseldin, H.E., Patel, N., Hashem, M., Ibrahim, N., Abdulwahab, F., et al. (2017). Clinical genomics expands the morbid genome of intellectual disability and offers a high diagnostic yield. Mol. Psychiatry *22*, 615–624.
22. Vissers, L.E.L.M., Gilissen, C., and Veltman, J.A. (2016). Genetic studies in intellectual disability and related disorders. Nat. Rev. Genet. *17*, 9–18.
23. Riazuddin, S., Hussain, M., Razzaq, A., Iqbal, Z., Shahzad, M., Polla, D.L., Song, Y., Beusekom, E., Van, and Khan, A.A. (2017). Exome sequencing of Pakistani consanguineous families identifies 30 novel candidate genes for recessive intellectual disability. Mol. Psychiatry *22*, 1604–1614.
24. Sobreira, N., Schiettecatte, F., Valle, D., and Hamosh, A. (2015). GeneMatcher: a matching tool for connecting investigators with an interest in the same gene. Hum. Mutat. *36*, 928–930.
25. Palombo, F., Graziano, C., Al Wardy, N., Nouri, N., Marconi, C., Magini, P., Severi, G., La Morgia, C., Cantalupo, G., Cordelli, D.M., et al. (2020). Autozygosity-driven genetic diagnosis in consanguineous families from Italy and the Greater Middle East. Hum. Genet. *139*, 1429–1441.
26. Petrovski, S., Gussow, A.B., Wang, Q., Halvorsen, M., Han, Y., Weir, W.H., Allen, A.S., and Goldstein, D.B. (2015). The Intolerance of Regulatory Sequence to Genetic Variation Predicts Gene Dosage Sensitivity. PLoS Genet. *11*, e1005492.
27. Ioannidis, N.M., Rothstein, J.H., Pejaver, V., Middha, S., McDonnell, S.K., Baheti, S., Musolf, A., Li, Q., Holzinger, E., Karyadi, D., et al. (2016). REVEL: An Ensemble Method for Predicting the Pathogenicity of Rare Missense Variants. Am. J. Hum. Genet. *99*, 877–885.
28. Wang, J., Al-Ouran, R., Hu, Y., Kim, S.Y., Wan, Y.W., Wangler, M.F., Yamamoto, S., Chao, H.T., Comjean, A., Mohr, S.E., et al.; UDN (2017). MARRVEL: Integration of Human and Model Organism Genetic Resources to Facilitate Functional Annotation of the Human Genome. Am. J. Hum. Genet. *100*, 843–853.
29. Kircher, M., Witten, D.M., Jain, P., O'Roak, B.J., Cooper, G.M., and Shendure, J. (2014). A general framework for estimating the relative pathogenicity of human genetic variants. Nat. Genet. *46*, 310–315.
30. Sim, N.L., Kumar, P., Hu, J., Henikoff, S., Schneider, G., and Ng, P.C. (2012). SIFT web server: predicting effects of amino acid substitutions on proteins. Nucleic Acids Res. *40*, W452-7.
31. Lek, M., Karczewski, K.J., Minikel, E.V., Samocha, K.E., Banks, E., Fennell, T., O'Donnell-Luria, A.H., Ware, J.S., Hill, A.J., Cummings, B.B., et al.; Exome Aggregation Consortium (2016). Analysis of protein-coding genetic variation in 60,706 humans. Nature *536*, 285–291.
32. Venselaar, H., Te Beek, T.A.H., Kuipers, R.K.P., Hekkelman, M.L., and Vriend, G. (2010). Protein structure analysis of mutations causing inheritable diseases. An e-Science approach with life scientist friendly interfaces. BMC Bioinformatics *11*, 548.
33. Riazuddin, S., Belyantseva, I.A., Giese, A.P.J., Lee, K., Indzhykulian, A.A., Nandamuri, S.P., Yousaf, R., Sinha, G.P., Lee, S., Terrell, D., et al. (2012). Alterations of the CIB2 calcium- and integrin-binding protein cause Usher syndrome type 1J and nonsyndromic deafness DFNB48. Nat. Genet. *44*, 1265–1271.
34. Gravotta, D., Carvajal-Gonzalez, J.M., Mattera, R., Deborde, S., Banfelder, J.R., Bonifacino, J.S., and Rodriguez-Boulan, E. (2012). The clathrin adaptor AP-1A mediates basolateral polarity. Dev. Cell *22*, 811–823.

35. Delevoye, C., Hurbain, I., Tenza, D., Sibarita, J.B., Uzan-Gafsou, S., Ohno, H., Geerts, W.J.C., Verkleij, A.J., Salamero, J., Marks, M.S., and Raposo, G. (2009). AP-1 and KIF13A coordinate endosomal sorting and positioning during melanosome biogenesis. J. Cell Biol. *187*, 247–264.
36. Ullrich, O., Reinsch, S., Urbé, S., Zerial, M., and Parton, R.G. (1996). Rab11 regulates recycling through the pericentriolar recycling endosome. J. Cell Biol. *135*, 913–924.
37. Grant, B.D., and Donaldson, J.G. (2009). Pathways and mechanisms of endocytic recycling. Nat. Rev. Mol. Cell Biol. *10*, 597–608.
38. Ren, X., Farías, G.G., Canagarajah, B.J., Bonifacino, J.S., and Hurley, J.H. (2013). Structural basis for recruitment and activation of the AP-1 clathrin adaptor complex by Arf1. Cell *152*, 755–767.
39. Bonifacino, J.S., and Traub, L.M. (2003). Signals for sorting of transmembrane proteins to endosomes and lysosomes. Annu. Rev. Biochem. *72*, 395–447.
40. Montpetit, A., Côté, S., Brustein, E., Drouin, C.A., Lapointe, L., Boudreau, M., Meloche, C., Drouin, R., Hudson, T.J., Drapeau, P., and Cossette, P. (2008). Disruption of AP1S1, Causing a Novel Neurocutaneous Syndrome, Perturbs Development of the Skin and Spinal. PLoS Genet. *4*, e1000296.
41. Ballarati, L., Cereda, A., Caselli, R., Maitz, S., Russo, S., Selicorni, A., Larizza, L., and Giardino, D. (2012). Deletion of the AP1S2 gene in a child with psychomotor delay and hypotonia. Eur. J. Med. Genet. *55*, 124–127.
42. Setta-Kaffetzi, N., Simpson, M.A., Navarini, A.A., Patel, V.M., Lu, H.C., Allen, M.H., Duckworth, M., Bachelez, H., Burden, A.D., Choon, S.E., et al. (2014). AP1S3 mutations are associated with pustular psoriasis and impaired Toll-like receptor 3 trafficking. Am. J. Hum. Genet. *94*, 790–797.
43. Janvier, K., Kato, Y., Boehm, M., Rose, J.R., Martina, J.A., Kim, B.Y., Venkatesan, S., and Bonifacino, J.S. (2003). Recognition of dileucine-based sorting signals from HIV-1 Nef and LIMP-II by the AP-1 γ-σ1 and AP-3 δ-σ3 hemicomplexes. J. Cell Biol. *163*, 1281–1290.
44. Jia, X., Singh, R., Homann, S., Yang, H., Guatelli, J., and Xiong, Y. (2012). Structural basis of evasion of cellular adaptive immunity by HIV-1 Nef. Nat. Struct. Mol. Biol. *19*, 701–706.
45. Yun, W.K., Hu, Y.M., Zhao, C.B., Yu, D.Y., and Tang, J.B. (2019). HCP5 promotes colon cancer development by activating AP1G1 via PI3K/AKT pathway. Eur. Rev. Med. Pharmacol. Sci. *23*, 2786–2793.
46. Tao, X., Lu, Y., Qiu, S., Wang, Y., Qin, J., and Fan, Z. (2017). AP1G1 is involved in cetuximab-mediated downregulation of ASCT2-EGFR complex and sensitization of human head and neck squamous cell carcinoma cells to ROS-induced apoptosis. Cancer Lett. *408*, 33–42.